

Field-induced ferromagnetic structure in $\text{Er}_2\text{Ni}_2\text{Pb}$

This article has been downloaded from IOPscience. Please scroll down to see the full text article.

2009 J. Phys.: Condens. Matter 21 216005

(<http://iopscience.iop.org/0953-8984/21/21/216005>)

View [the table of contents for this issue](#), or go to the [journal homepage](#) for more

Download details:

IP Address: 129.252.86.83

The article was downloaded on 29/05/2010 at 19:55

Please note that [terms and conditions apply](#).

Field-induced ferromagnetic structure in $\text{Er}_2\text{Ni}_2\text{Pb}$

K Prokeš¹ and J A Mydosh^{2,3}

¹ Helmholtz-Zentrum Berlin für Materialien und Energie, SF-2, Glienicker Straße 100, D-14109 Berlin, Germany

² Institute of Physics II, University of Cologne, D-50937 Cologne, Germany

³ Kammerlingh Onnes Laboratory, Leiden University, 2300 RA Leiden, The Netherlands

E-mail: prokes@helmholtz-berlin.de and mydosh@ph2.uni-koeln.de

Received 1 December 2008, in final form 8 April 2009

Published 30 April 2009

Online at stacks.iop.org/JPhysCM/21/216005

Abstract

We have studied the effect of magnetic fields up to 4.5 T on the ground-state structure in $\text{Er}_2\text{Ni}_2\text{Pb}$ using powder neutron diffraction measurements at low temperatures. The zero-field magnetic state that itself is not uniform and consists of different magnetic phases is rather unstable against the magnetic field. As the field is increased, the magnetic reflections of the zero-field structure disappear and a new magnetic phase with commensurate propagation vector is clearly observed in a field of 0.5 T. At higher fields a ferromagnetic state is established in $\text{Er}_2\text{Ni}_2\text{Pb}$, which can be fully described only by a model that combines at least two irreducible representations. The refined Er magnetic moment magnitude of $9.10 \pm 0.07 \mu_B$ is very close to the Er^{3+} free ion value of $9.0 \mu_B$.

(Some figures in this article are in colour only in the electronic version)

1. Introduction

A few years ago a new large family of $\text{R}_2\text{Ni}_2\text{Pb}$ (R stands for Y, Nd and from Gd to Lu) intermetallic isostructural compounds was synthesized and studied by various groups [1–3]. Magnetic bulk measurements showed that the only magnetic element in these materials is the rare-earth ion [4]. To our knowledge, only three of the systems (containing Dy [5], Ho [6] and Er [7]) have been studied to date by means of the powder neutron diffraction technique. The determined magnetic structures are highly unusual and interesting.

All the compounds crystallize in the orthorhombic Mn_2AlB_2 type (sometimes denoted as the AlB_2Fe_2) crystal structure [1]. All the R atoms occupy the same crystallographic position and are equivalent in the crystal structure. An interesting point is that the Er atoms form two chains each consisting of a nearly triangular net. Four Er–Er bonds can be clearly identified in the structure: 1, along the b axis the Er–Er separation equals 3.883 Å; 2, the link that is almost along the [110] direction amounts to 3.6612 Å and 3, that between the Er atoms along the a axis is 4.004 Å long. Finally, 4, the distance between the Er atoms along the c axis, amounts to 3.61 Å. The largest relative difference between the Er distances within the a – b plane is 9%. It is clear that such geometry can lead

to competing magnetic interaction frustration effects leading in $\text{Er}_2\text{Ni}_2\text{Pb}$ to a large variety of different antiferromagnetic structures. Previous bulk magnetic measurements [4, 8] suggested three magnetic phase transitions at $T_{\text{N}1} = 3.4$ K, $T_{\text{N}2} = 3.2$ K and $T_{\text{N}3} = 2.0$ K to exist in $\text{Er}_2\text{Ni}_2\text{Pb}$. Neutron diffraction experiments down to 1.5 K [7] and 460 mK [9] proved all the magnetic phases to be antiferromagnetic and coexisting over an extended temperature range. It is striking that the two experiments revealed different phase transition temperature values. We have found it equally striking that the low temperature state is not uniform and consists of spatially separated magnetic phases, one of them being incommensurate with the crystal structure. The two neutron experiments also led to different fractional volumes of the relevant phases. Last but not least, the incommensurate phase with propagation vector $q = (0.470\ 1/2)$, that seemed to be unstable in one experiment, appeared to be stabilized down to 460 mK in the second one. It has not been proved or disproved [9] whether it is a transversal sine-wave modulated magnetic structure or a spin-slip structure derived from an originally commensurate structure with propagation vector $q = (1/2\ 0\ 1/2)$. The former phase should be unstable in the low temperature limit. From entropy arguments it follows that a squaring-up should occur at finite temperature and the spin-slip structure seems to be more

Table 1. Structural parameters of $\text{Er}_2\text{Ni}_2\text{Pb}$ determined above the magnetic phase transition (in the paramagnetic state) at 5 K before the application of a magnetic field of 4.5 T using powder neutron diffraction. The fitted results obtained after applying the field are very similar.

Space group		$Cmmm$			
Para, $T = 5$ K					
Atom	Site	Pos. Param.	B (Å)	Occupation	
Er	4j	0, 0.3568 (5), $\frac{1}{2}$	0.1 (fixed)	1.00 (fixed)	
Ni	4i	0, 0.1979 (4), 0	0.1 (fixed)	0.984 (fixed)	
Pb	2a	0, 0, 0	0.1 (fixed)	0.976 (fixed)	
Lattice constants (Å)		$a = 4.002$ (2)	$b = 13.864$ (7)	$c = 3.607$ (3)	
Agreement factors		$R_p = 4.36\%$	$R_B = 6.82\%$		

probable. However, why such a spin-slip structure would be more stable than the commensurate one remains unclear. We have argued that the geometrical arrangement of Er moments leading to competing interactions combined with structural defects is responsible for these remarkable observations [7]. One has to note that both experiments have been performed on the same sample. The only difference is that the sample has been exposed for a long time to air.

One of the main aims of the present experiment which was performed shortly after the first experiment was to derive the Er moment magnitude by forcing the $\text{Er}_2\text{Ni}_2\text{Pb}$ to be ferromagnetic. This can be done by a relatively low magnetic field of about 2 T [4, 8]. The other purpose was to check how stable are the zero-field magnetic structures upon application of a magnetic field.

2. Experimental details

The sample used in the present study is the same one as used for the other two neutron experiments [7, 9]. Preparation and magnetic characterization details can be found in [8]. Neutron diffraction patterns were collected at selected temperatures between 1.6 and 5 K using the multicounter diffractometer E6 installed at the Helmholtz Centre, Berlin. The incident-neutron wavelength was 2.44 Å. A superconducting cryomagnet capable of generating 4.5 T has been employed to achieve low temperatures and to apply the magnetic field. For these measurements about 6 g of $\text{Er}_2\text{Ni}_2\text{Pb}$ was encapsulated inside a vanadium container and pressed together to minimize realignment of the grains due to the applied magnetic field. The data were collected for 6 h at each of the selected temperatures in zero field before the application of the magnetic field, then in a magnetic field of 4.5 T keeping the temperature at 1.67 K and finally again in zero field with increasing the temperature up to 5 K. Besides that, we have followed a small portion of the diffractogram between 30° and 50° as a function of magnetic field at 1.67 K when increasing the field from zero to 4.5 T. In this case the counting time was about 1 h. The data were analyzed by means of the Rietveld profile procedure [10] using the computer code FULLPROF which is part of a larger package Winplotr [11]. The Er magnetic form factor was taken from [12]. All the diffraction data were corrected for substantial absorption.

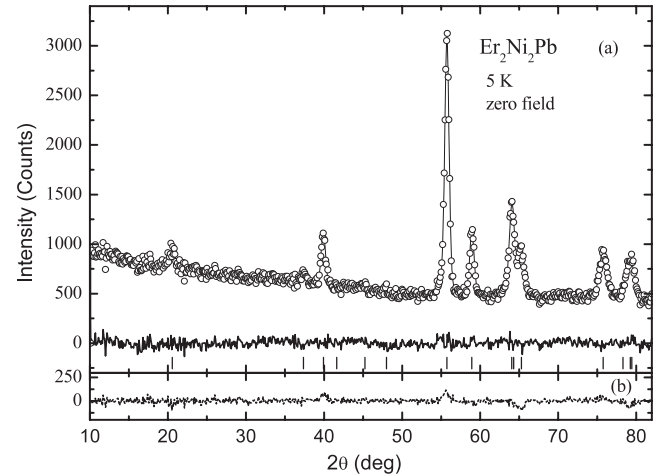


Figure 1. (a) The diffraction data (circles) of $\text{Er}_2\text{Ni}_2\text{Pb}$ taken in zero field at 5 K after application of 4.5 T together with the best fit (the full line through points) and the difference between them (line at the bottom). The positions of the magnetic Bragg reflections are tick-marked at the bottom. The diffraction pattern taken at identical conditions, however, before the application of the magnetic field is virtually identical. For numerical results see table 1. (b) The difference between the pattern recorded before and after the application of a magnetic field of 4.5 T on the closely packed $\text{Er}_2\text{Ni}_2\text{Pb}$ powder sample.

3. Results

3.1. Paramagnetic state

The systematic extinction of reflections in the powder neutron diffraction pattern recorded at 5 K in the paramagnetic state conforms completely with the space group $Cmmm$. The best refinement leads to results that are in very good agreement with structural parameters reported for this compound in the literature [1, 7]. All the Er atoms in the unit cell occupy the 4j position at 0, y_{Er} , $\frac{1}{2}$ with the local symmetry $m2m$ and are crystallographically equivalent. Ni atoms occupy 4i positions at 0, y_{Ni} , 0 and Pb atoms the 2a Wyckoff position 0, 0, 0. There are four Er atoms in the crystallographic unit cell. As in our last work we denote the corresponding atomic positions as Er_1 at 0, 0.3603, $\frac{1}{2}$, Er_2 at 0, 0.6397, $\frac{1}{2}$, Er_3 at $\frac{1}{2}$, 0.8603, $\frac{1}{2}$ and Er_4 at $\frac{1}{2}$, 0.1397, $\frac{1}{2}$. The paramagnetic space group $Cmmm$ symmetry operations include a $(\frac{1}{2}, \frac{1}{2}, 0)$ translation. Due to the lower number of reflections observed we kept the isotropic Debye–Waller factor for all three atoms equal to 0.1 Å. Numerical values of the best fit are summarized in table 1.

The best fit to data also taken at 5.0 K, however, after application of 4.5 T suggests that the redistribution of grains due to magnetic field was rather small during the experiment. To document this we show at the bottom of figure 1 the difference between the diffractogram taken before and after the application of the magnetic field. However, in order to account even for such small changes in preferential orientation we have defined several reciprocal directions and fitted the parameter describing it. Results of a comprehensive effort suggests that a small portion of crystallites realigned along a direction close to, but not identical to, the b axis. The diffraction pattern taken

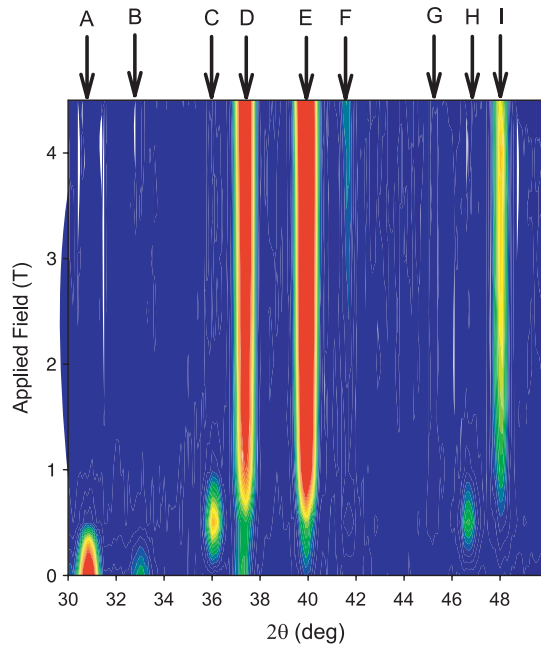


Figure 2. Contour intensity plot showing small-angle portion of diffraction patterns taken on $\text{Er}_2\text{Ni}_2\text{Pb}$ with increasing applied magnetic field. The nine Bragg reflections denoted by arrows and capital letters A · · · I are discussed in the text.

after the application of the magnetic field together with the best fit to data is shown in figure 1.

3.2. Magnetically ordered states in zero field

Refinement of zero-field data taken at 3.0, 2.5, 2.0 and 1.67 K, the lowest temperature of this experiment, led to results that are in very good agreement with previous experiments [7, 9]. This holds for a magnetic state just below the $T_N = 3.4$ K that is described by the propagation vector $q_1 = (0.8400.5)$ and the magnetic state that exists at 2.5 K and consists of two magnetic phases (described by q_1 and $q_2 = (0.5900.5)$). Even for the magnetic state existing at 2.0 K, where besides magnetic phases described by q_1 and q_2 propagation vectors, the third magnetic structure described by the propagation vector $q_3 = (0.4700.5)$ exists, identical results have been obtained. The only difference is a slightly different volume percentage of various phases at the lowest temperature, at 1.67 K. In the case of the experimental results described in [9] the volume fraction was 54%, 6% and 40% for the magnetic phase described by q_3 , $q_{4-1} = (0.50.50.5)$ and $q_{4-2} = (000.5)$ propagation vector, respectively. In the present case we found for these three coexisting magnetic phases a population 51%, 3% and 46%. In the calculation it was supposed that the magnetic moment magnitude is equal in all phases. In that case it amounts to $7.7 \mu_B/\text{Er}$.

3.3. Influence of the applied magnetic field at 1.67 K

In figure 2 we show an interpolated contour intensity resulting from nine short-time scans measured with increasing magnetic field. For the sake of clarity and discussion we label them by

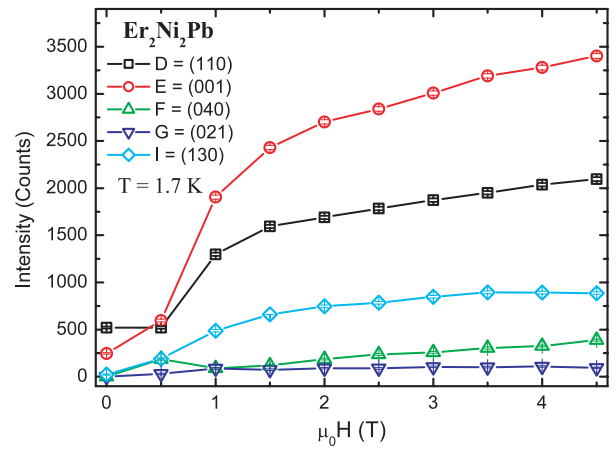


Figure 3. Field dependence of the nuclear Bragg peak integrated intensities extracted from data shown in figure 2.

capital letters A · · · I. Reflections that exist in zero field are easy to identify. The two strongest zero-field reflections in this scattering range, the A and B reflections, are composed from four symmetry related reflections of the $(0.51.50.5) = (010)^{+q_4-1}$ and $(0.4720.5) = (020)^{+q_3}$ type, respectively. The other two that are clearly visible in zero field are reflections D and E. While reflection E is a pure nuclear (001) reflection, the former reflection D consists of the nuclear reflection (110) and a composite of four equivalent reflections of the type $(0.52.50.5) = (020)^{+q_4-1}$. In the given range there are three other nuclear reflections that are barely visible in figure 2 in zero-field conditions: reflection F = (040) , G = (021) and reflection I = (130) .

The two remaining reflections C and H exist only in a very narrow field range and cannot be indexed with any of the known propagation vectors so far. However, from a comparison with data taken in zero field at 3 K it appears that they are very close to reflections indexable with propagation vector $q_1 = (0.8400.5)$. Two C and H reflections are indexable with commensurate propagation vector $q_5 = (5/600.5)$. They are identified as being composed of three reflections of the type $(000)^{+q_5} = (0.83300.5)$ in the case of the C reflection and four reflections of the type $(141)^{-q_5} = (0.16740.5)$ and one $(200)^{-q_5} = (1.1670-0.5)$ for reflection H. It is not the subject of the present work to refine the details of the magnetic state existing in a very narrow field range around 0.5 T. We only wish to note that the arrangement of the magnetic moments should be very similar to the transverse-modulated magnetic structure existing just below the antiferromagnetic phase transition and which was determined in [7].

3.4. Field-induced ferromagnetic structure

Starting from zero field, i.e. even in the range where the q_5 magnetic structure exists, all the nuclear reflections (except for reflection D) increase in intensity (see figure 3). At first the intensity increase is rather moderate but above the field where the q_5 magnetic structure starts to disappear they do increase substantially. Reflection D, which consists of nuclear reflection

Table 2. Transformation rules for magnetic moment components of possible magnetic structure models belonging to different irreducible representations Γ that are in accord with the position $4j$ site of the $Cmmm$ space group and the magnetic propagation vector q_6 and q'_6 . Sequence ‘+ - + -’ for $M(x_1x_2x_3x_4)$ denotes that the x component at the Er_1 site is coupled parallel to the x component at the Er_3 site and antiparallel to those at Er_2 and Er_4 . Zero denotes that no such component is allowed.

$T = 1.67 \text{ K } B = 4.5 \text{ T}$		Γ_1	Γ_2	Γ_3	Γ_4	Γ_5	Γ_6	Γ_7	Γ_8
$q_6 = (000)$	$M(x_1x_2x_3x_4)$	0000	0000	++++	0000	0000	0000	0000	+ - + -
	$M(y_1y_2y_3y_4)$	0000	+ - + -	0000	0000	++++	0000	0000	0000
	$M(z_1z_2z_3z_4)$	0000	0000	0000	+ - + -	0000	0000	++++	0000
$q'_6 = (010)$	$M(x_1x_2x_3x_4)$	0000	0000	+- - -	0000	0000	0000	0000	+ - - +
	$M(y_1y_2y_3y_4)$	0000	+ - - +	0000	0000	+- - -	0000	0000	0000
	$M(z_1z_2z_3z_4)$	0000	0000	0000	+ - - +	0000	0000	+ - - -	0000

(1 1 0) and zero-field AF reflections, shows a plateau and starts to increase only after the q_5 reflections disappear. Reflections $F = (040)$, $G = (021)$ and $I = (130)$, which in zero field virtually do not exist, are clearly visible in the 4.5 T pattern. A very strong increase in intensity is observed for reflection $E = (001)$ —by a factor of 25 or so. The only reflection that remains rather small in the field of 4.5 T is reflection $G = (021)$. We interpret, in agreement with the magnetization data [4] and the fact that it was proven that the powder grains did not reorient themselves substantially, the increase of the intensity of these reflections as being due to the ferromagnetic order of Er moments that is produced by an external magnetic field.

All the reflections visible in 4.5 T are indexable with integer indices. This suggests that the magnetic unit cell is of the same size as the crystallographic one. In other words, the propagation vector of such a magnetic structure is either $q_6 = (000)$ or $q'_6 = (010)$. Possible magnetic structures compatible with the $Cmmm$ space group and q_6 or q'_6 propagation vectors have been generated by using the computer code MODY [13] based on the symmetry analysis. These are presented in table 2. As can be seen, for the propagation vector q_6 there are only three irreducible representations (IR) that allow for ferromagnetic alignments of Er moments. These are denoted as Γ_3 (moments along the a axis), Γ_5 (moments along the b axis) and Γ_7 (moments along the c axis). For the propagation vector q'_6 there is no ferromagnetic moment alignment possible.

From the above-mentioned experimental findings and from a direct comparison of the datasets taken at low temperature in zero field and in 4.5 T, which also show an increase of the (2 0 0) reflection, it follows that the Er moments cannot be directed solely along one of the three principal axes. Such is excluded because of the increase of the (2 0 0), (0 0 1) and (0 4 0) reflections at the same time. This suggests that we are dealing with a mixing of at least two IRs. Let us note that the mixing of different irrep IRs is not that common, as only one type of magnetic fluctuations that is in accord with the symmetry of the Hamiltonian above the magnetic phase transition develops into stable magnetic moments at lower temperatures. Several examples are known in the literature [14]. In addition, here we are dealing with a field-induced state that introduces a new symmetry axis into the problem. In order to get a feeling of how significant the mixing of different IRs could be, we have performed a series of fits to pure (i.e. originating from a single IR) models. The

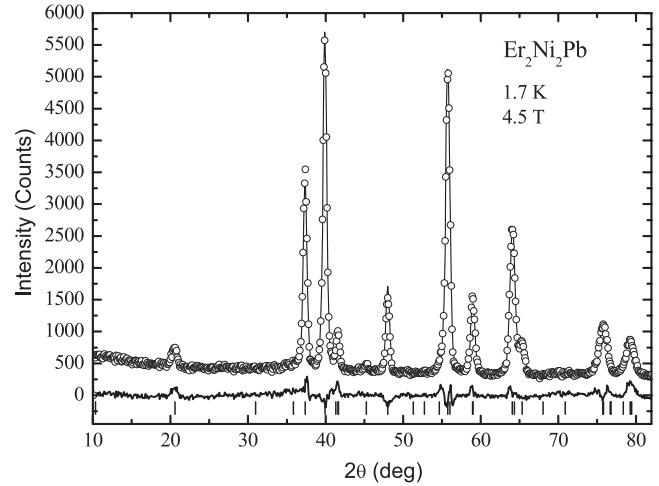


Figure 4. The diffraction data (circles) of Er_2Ni_2Pb taken in 4.5 T at 1.7 K together with the best fit (the full line through points) to the model following from the combination of $\Gamma_3 + \Gamma_5$ IRs and the difference between them (line at the bottom). The positions of the magnetic Bragg reflections are tick-marked at the bottom. The model fit that combines Γ_3 , Γ_5 and Γ_7 IRs gives identical quality fits. For numerical results see table 1.

fit supposing moments solely aligned along the a and c axes lead to moment magnitudes of $8.0 \pm 0.1 \mu_B$ and $6.7 \pm 0.1 \mu_B$ and miss the intensity of the (2 0 0) and (0 0 1) reflection, respectively. The best fit of the ferromagnetic model with Er moments along the b axis to the experimental data leads to a moment magnitude of $8.59 \pm 0.08 \mu_B$ and, of course, to zero intensity on the (0 4 0) reflection.

To account for the observed diffraction pattern correctly, one has to combine at least two of the models given in table 2 belonging to different irreducible representations. Satisfactory agreement has been found for models following from Γ_3 and Γ_5 IRs (see figure 4). In this case, the best fit leads to Er moment magnitudes of $9.10 \pm 0.07 \mu_B$, a value that is in good agreement with the Er^{3+} free ion value. The best fit to a model that is constructed from all three ferromagnetic models belonging to Γ_3 , Γ_5 and Γ_7 IRs leads to a moment magnitude that is not that different: $9.15 \pm 0.08 \mu_B$. Numerical results are summarized in table 3. Although the quality of both fits is nearly identical and one can hardly distinguish between them, individual Cartesian moment components are rather different.

Table 3. Magnetic parameters of Er₂Ni₂Pb determined at 1.67 K and 4.5 T using powder neutron diffraction. The total moment has been calculated with the assumption that the magnetic structure is uniform in the whole volume of the sample.

Er moment IR	x component $\mu_x (\mu_B)$	y component $\mu_y (\mu_B)$	z component $\mu_z (\mu_B)$	Total $\mu_z (\mu_B)$
$\Gamma_3 + \Gamma_5$	5.29 (13)	7.41 (10)	0	9.10 (7)
Agreement factors	$R_p = 6.04\%$	$R_B = 6.84\%$	$R_M = 6.37\%$	
$\Gamma_3 + \Gamma_5 + \Gamma_7$	5.58 (14)	6.51 (20)	3.19 (27)	9.15 (8)
Agreement factors	$R_p = 5.91\%$	$R_B = 6.76\%$	$R_M = 6.74\%$	

4. Discussion

The present neutron diffraction results clearly show that the stability of the zero-field low temperature magnetic structure in Er₂Ni₂Pb is very limited. It can be modified by magnetic fields as low as 0.5 T and forced to be ferromagnetic above 1.5–2 T. Our powder neutron diffraction results show unambiguously that above this field the magnetic state of Er₂Ni₂Pb is ferromagnetic.

Naturally, one has to be cautious when dealing with data obtained on polycrystalline samples that are exposed to a magnetic field. In particular, the analysis and interpretation has intrinsic limitations due to averaging over statistically distributed directions of powder grains. However, we believe that semiquantitative information can still be obtained and interpreted. The use of single crystals would lead to ‘clean’ and direct information regarding the field dependence of integrated intensities of individual reflections. However, their number would be greatly limited by the geometry constraints of the experiment. Powder experiments yield moment directions that are averaged over all possible crystallite orientations with respect to the applied magnetic field. Using tiny single-crystal magnetization measurements [4] revealed the *a* and the *b* axes of Er₂Ni₂Pb are the easy magnetization axes. Two metamagnetic-like transitions at about 0.25 and 1.5 T for a field along the *b* axis and one around 1.5 T along the *a* axis are found at 1.8 K [4]. The magnetization values of $\mu_a = 6$ and $\mu_b = 8 \mu_B/\text{Er}$ found for the *a* and *b* axes orientation at 3 T are nearly an order of magnitude larger than that one along the *c* axis. The *c* axis shows no transition up to at least 10 T and it is therefore considered as the hard magnetization axis. The Er₂Ni₂Pb has thus a easy plane type of magnetocrystalline anisotropy. As discussed in [15], which deals with the same type of experiment but on another material, for an ideal ferromagnetic material for which two crystallographic axes are equally easy directions and the remaining axis is much harder, one expects that the magnetic moments will be fully aligned within the easy magnetization plane along the projection of the applied field onto this plane. This scenario disqualifies in our case the model combining all three ferromagnetic IRs. A powder measurement averaged over all crystallite orientations should show an average moment direction pointing at 45° between the two easy magnetization directions. Our data that are summarized in table 3 suggest that this angle is slightly different. It amounts to $\zeta_{(4.5\text{T})} = \arccos(\mu_x/\mu_{\text{tot}}) = \arctan(\mu_y/\mu_x) = \text{atan}(7.41/5.29) = 54.5^\circ$ with respect to the *a* axis and $90 - \zeta = 35.5^\circ$ with respect to the *b* axis. This corresponds very well to the ratio of magnetizations found at 3 T on the single crystal $\zeta'_{(3\text{T})} = \text{atan}(\mu_b/\mu_a) = \text{atan}(8/6) =$

53.2°. If one compares these angles with crystal structure parameters one realizes that $\zeta_{(4.5\text{T})}$ is also (within the error bars) identical to the angle that makes the link between the Er₁ atom at (0, y_{Er} , 0.5) and the Er₄ atom at (0.5 0.5 – y_{Er} 0.5) with the *a* axis and which amounts to 56°. It is therefore tempting to conclude that the anisotropy within the *a*–*b* plane (if it indeed exists) favors the alignment of Er moments along such links. This, however, needs to be confirmed by performing neutron diffraction on a single crystal.

One can try to interpret the data with just the opposite assumption. Let us suppose that one deals with a spatially inhomogeneous magnetic state that consists from ferromagnetic domains in which the magnetic state is described by Γ_3 (moments along the *a* axis) and regions in which the Γ_5 (moments along the *b* axis) exist. Let us further suppose an identical magnetic moment in both. Then, exactly 1/3 of the volume would be in the Γ_3 state and 2/3 in the Γ_5 state. The volume fraction of the two domains would then depend on the orientation of crystallites with respect to field and inevitably leads to uniform and equal magnetization along the *a* and *b* axes if measured on a single crystal. Such a model is, however, in disagreement with magnetization measurements [4] mentioned above. A model that considers their experimental and unequal values is not feasible as both values are smaller than $9 \mu_B/\text{Er}$, a value determined from neutron diffraction data. Therefore, it seems to be quite probable that the anisotropy within the *a*–*b* plane locks the Er magnetic moments along the Er₁–Er₄ or equivalent links. Single-crystal work is indispensable here.

5. Conclusion

We have presented the results of neutron diffraction measurements at low temperatures and in fields up to 4.5 T performed on closely packed powders of Er₂Ni₂Pb. It has been shown that the zero-field magnetic structure is rather unstable against the magnetic field. The magnetization process is not simple. A new magnetic phase with commensurate propagation vector is clearly observable in a field of 0.5 T. At higher fields a ferromagnetic state is established in Er₂Ni₂Pb, which can be described by a model that combines two irreducible representations. The refined Er magnetic moment magnitude of $9.10 \pm 0.07 \mu_B$ is very close to the Er³⁺ free ion value of $9.0 \mu_B$.

Acknowledgment

KP would like to thank the ILL for its hospitality during his short leave from HZB.

References

- [1] Gulay L D, Kalychak Y M and Wolcyrz M 2000 *J. Alloys Compounds* **311** 228
- [2] Muñoz-Sandoval E, Chinchure A D, Hendrikx R W A and Mydosh J A 2001 *Europhys. Lett.* **56** 302
- [3] Goruganti V, Li Y, Ross J H Jr, Rathnayaka K D D and Öner Y 2006 *J. Appl. Phys.* **99** 08P303
- [4] Chinchure A D, Muñoz-Sandoval E and Mydosh J A 2002 *Phys. Rev. B* **66** 020409
- [5] Prokeš K, Muñoz-Sandoval E, Chinchure A D and Mydosh J A 2003 *Phys. Rev. B* **68** 134427
- [6] Prokeš K, Muñoz-Sandoval E, Chinchure A D and Mydosh J A 2005 *Eur. Phys. J. B* **43** 163
- [7] Prokeš K, Muñoz-Sandoval E, Chinchure A D and Mydosh J A 2008 *Phys. Rev. B* **78** 014425
- [8] Chinchure A D, Muñoz-Sandoval E and Mydosh J A 2001 *Phys. Rev. B* **64** 020404(R)
- [9] Prokeš K and Mydosh J A 2009 *Eur. Phys. J. B* **67** 1
- [10] Rietveld H M 1969 *J. Appl. Crystallogr.* **2** 65
- [11] Roisnel T and Rodríguez-Carvajal J 2001 *Mater. Sci. Forum* **378** 118
- [12] Sears V F 1992 *Neutron News* **3** 26
- [13] Sikora W, Bialas F, Pytlik L and Malinowski J 2004 *J. Appl. Crystallogr.* **37** 1015
- [14] Kenzelmann M, Harris A B, Jonas S, Broholm C, Schefer J, Kim J B, Zhang C L, Cheong S-W, Vajk O P and Lynn J W 2005 *Phys. Rev. Lett.* **95** 087206
- [15] Wilson N R, Petrenko O A and Chapon L C 2007 *Phys. Rev. B* **75** 094432